Geometric Determination of the Dexterous Workspace of n-RRRR and n-RRPR Manipulators

André Gallant[a], Roger Boudreau[a,*], Marise Gallant[a]

[a]*Département de génie mécanique, Université de Moncton, 18 ave Antonine-Maillet, Moncton, N. B., Canada E1A 3E9*

Abstract

In this work, a geometric method is presented to determine the dexterous workspace of two architectures of kinematically redundant planar parallel manipulators. The architectures studied are n-RRRR and n-RRPR[1] . These architectures are characterized by having a revolute actuator as the kinematically redundant actuator added to the base of each kinematic chain. First, the dexterous workspace of the non-redundant part (RRR or RPR) of each kinematic chain is studied. Then the effect of the redundant actuator is considered to yield a geometric representation of the dexterous workspace of each kinematic chain. The intersection of the dexterous workspaces of all kinematic chains of a manipulator is determined to obtain the geometric representation of the dexterous workspace. Finally, the Gauss Divergence Theorem is applied to compute the area of the dexterous workspace. An example is given to demonstrate an application of the method.

Keywords: kinematic redundancy, planar parallel manipulator, dexterous workspace, RRRR, RRPR

*Tel.:1 506 858 4373, Fax.: 1 506 858 4082

Email addresses: eag3440@umoncton.ca (André Gallant), roger.a.boudreau@umoncton.ca (Roger Boudreau), marise.gallant@umoncton.ca (Marise Gallant)

[1]The parallel manipulators considered consist of n serial kinematic chains that connect the end-effector to the base. R indicates a revolute joint and P indicates a prismatic joint. Underlined letters in the notation indicate that the joint is actuated.

1. Introduction

An important characteristic of a parallel manipulator is its workspace. Several types of workspace have been proposed, such as the constant orientation workspace, the maximal workspace, the inclusive maximal workspace, and the dexterous workspace [1, 2]. The dexterous workspace for planar manipulators is certainly one of the most useful. This type of workspace represents the region that can be attained by the reference point on the end-effector with any orientation.

Several researchers have studied the dexterous as well as other types of workspace for the non-redundant 3-RRR symmetric planar architecture [1, 3, 4]. The dexterous workspace in these works was defined by a maximum of two concentric circles for each of the three kinematic chains. The radius of the outer circle corresponded to the configuration when the two links attached to the base are fully stretched out, while the inner radius corresponded to the configuration when they are fully folded. Zhaohui and Zhonghe [5] identified a third concentric circle near the base of each kinematic chain by using the four-bar mechanism analogy on a symmetric 3-RRR manipulator. Various workspaces of the 3-RRR and the 3-RPR manipulators were determined in [2]. Several works, see for example [3, 6], have determined the surface area of different types of workspaces by integration of the workspace boundary based on the Gauss Divergence Theorem [7].

Redundancy was introduced in parallel manipulators [8, 9, 10, 11, 12] to alleviate some of their disadvantages when compared to serial manipulators, e.g., to enlarge their workspaces or to eliminate singular configurations within their workspaces. Redundancy can be classified either as actuation redundancy or as kinematic redundancy. The former consists of actuating some of the passive joints while the latter consists of adding extra active joints and links.

Ebrahimi et al. [13, 14] introduced new kinematically redundant manipulators by adding an actuated prismatic actuator to the base of each kinematic chain of the 3-RRR and by adding an actuated revolute joint to the base of each chain of the 3-PRR manipulator architectures. The dexterous workspace of these kinematically redundant manipulators was obtained with a discreet method which is computationally inefficient and does not yield an exact solution.

The determination of the dexterous workspace of planar n-RRRR and n-RRPR manipulators, or of hybrid n-RRRR-m-RRPR manipulators, is the

object of this work. A method similar to the one presented in this work was applied to the n-PRRR manipulator [15, 16]. In what follows, in order to alleviate the text, the term workspace will denote the dexterous workspace.

2. Architectures

In Figure 1, examples of the architectures studied are illustrated. Figure 1(a) shows an example 3-RRRR manipulator whereas Figure 1(b) shows an example 3-RRPR manipulator. In these figures, solid circles indicate an actuated revolute joint while a hollow circle indicates a passive revolute joint. It can be seen that the n-RRRR and the n-RRPR manipulators are based on the well known 3-RRR and 3-RPR manipulators, respectively. In both of these manipulator architectures, an actuated revolute joint and a link are added to the base of each kinematic chain. As will be shown later, the workspaces of the 3-RRR and 3-RPR manipulators both consist of up to three concentric circles, producing dexterous workspaces for the redundant manipulators that are similar.

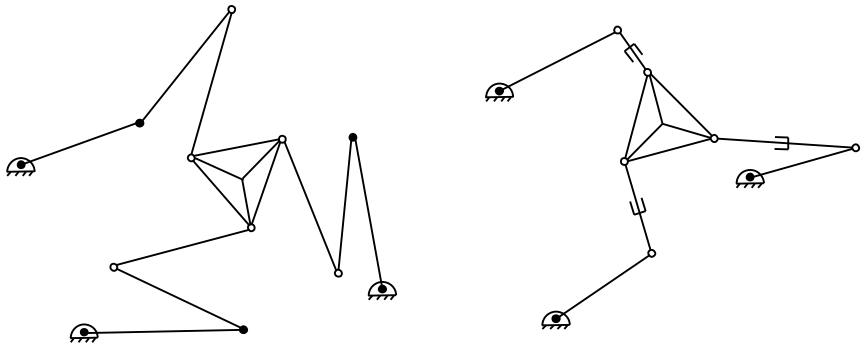

(a) 3-RRRR (b) 3-RRPR

Figure 1: Example 3-RRRR and 3-RRPR planar parallel manipulators

3. Methodology

It is well known that for a parallel manipulator, its workspace is the intersection of the workspaces of each branch. The basic concepts of the method described in this work can be applied to many different planar parallel architectures. The method can be summarized by the following five steps:

1. Determine the boundaries of the workspace of each kinematic chain.
2. Determine all points of intersection between the boundaries of the workspace of each kinematic chain with all the other chains.
3. Segment the boundaries of the workspace of each kinematic chain at each of their points of intersection.
4. Determine which of these segments are part of the boundaries of the workspace of the manipulator, i.e., intersect all other kinematic chains.
5. Compute the contribution of each segment in the workspace and add them to obtain the area of the workspace of the manipulator.

The first four steps yield a geometric representation of the workspace while the fifth step yields a scalar value for the area of the workspace in units of length squared. In this section, each of these steps, as applies to the n-RRRR and n-RRPR manipulator architectures, is explained further.

Step 1 in the method to obtain the workspace of these manipulator architectures is to determine the boundaries of the workspace of each kinematic chain. For this, the workspace of the non-redundant part only of each kinematic chain architecture can first be determined. The effect of the redundant actuator can be considered afterwards to determine the boundaries of the workspace for each redundant kinematic chain.

3.1. Workspace of RRR Kinematic Chains

The first architecture to be studied is the RRR non-redundant portion of the RRRR kinematic chain. Figure 2 shows an example RRR kinematic chain, where (X_1, Y_1) are the coordinates of the base of the kinematic chain and (X_2, Y_2) are the coordinates of the end-effector. The length of the proximal link is denoted by L_1, L_2 is the length of the distal link, and L_3 is the length of the link that connects the distal link to the end-effector (represents the platform). Finally, L_0 is the distance separating (X_1, Y_1) and (X_2, Y_2) for a given posture. It can be seen that (X_1, Y_1), L_1, L_2, and L_3 are constant, whereas (X_2, Y_2) and L_0 vary with the position of the end-effector.

The analysis presented in [15], where a four-bar mechanism analogy is utilized, is briefly summarized here. The workspace for RRR kinematic chains is defined by one, two or three concentric circles, depending on the relationships between the constant link lengths L_1, L_2 and L_3. Shapes of the workspaces were defined as classes. These classes are shown in Figure 3 where it can be seen that the workspace of RRR kinematic chains is comprised of one, two or three concentric circles defining a workspace of Class 1, 2 or 3, respectively.

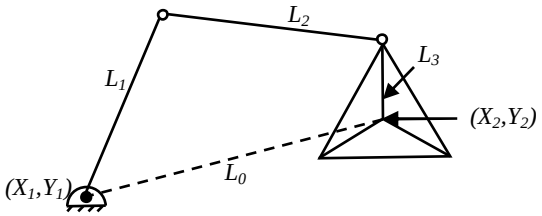

Figure 2: Example RRR kinematic chain

The radius of each concentric circle, defined by r_1, r_2 or r_3, are determined using the following relationships between the constant link lengths [15]:

$$\begin{aligned} r_1 &= S + M - L \\ r_2 &= |L_1 - L_2| + L_3 \\ r_3 &= L_1 + L_2 - L_3 \end{aligned} \tag{1}$$

where S is the length of the shortest link, L is the length of the longest link and M is the length of the other link.

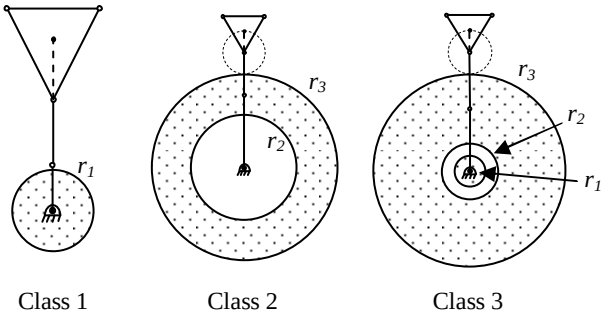

Figure 3: Workspace classes for RRR kinematic chains

The concept behind the method used to determine these classes is that for a given end-effector position, if the link of length L_3 is a crank, in the four-bar mechanism analogy, that position is part of the workspace of the non-redundant kinematic chain. When the position of the end-effector changes, the length L_0 changes and at specific lengths, the resulting four-bar mechanism changes category. For example, when all the links are stretched out, L_0 becomes the longest link. The mechanism becomes a triple rocker and the region is outside the dexterous workspace since the end-effector cannot

complete a full revolution. As the end-effector is moved closer to the fixed revolute joint, L_0 becomes shorter, and the mechanism's category can change to a crank rocker or a double crank, depending on the link lengths. When the mechanism belongs to one of these categories, with L_3 as the crank, the end-effector is in the workspace. Thus, finding the lengths L_0 that permit L_3 to be a crank forms circles that define the workspace of the non-redundant kinematic chain. Table 1 shows the conditions under which each concentric circle defines a boundary of the workspace of the RRR kinematic chain.

Table 1: Conditions for each RRR kinematic chain class [15]

	No link longer than sum of others	**One link longer than sum of others**
$\boldsymbol{L_3}$ **shortest**	Class 3 (r_1, r_2 and r_3)	Class 2 (r_2 and r_3)
$\boldsymbol{L_3}$ **not shortest**	Class 1 (r_1)	No workspace

In this table, it can be seen that the class of the workspace depends on the shortest link and on whether or not any link is longer than the sum of the two others.

3.2. Workspace of RPR Kinematic Chains

The n-RRPR architecture is based on the 3-RPR manipulator with a revolute redundant actuator added at the base of each kinematic chain. Again, the non-redundant portion of the kinematic chain can be studied separately from the effect of the redundant actuator. An example RPR kinematic chain is shown in Figure 4 where L_1 is the length of the prismatic actuator for a given posture, and L_1^{min} and L_1^{max} are the minimum and maximum lengths of the prismatic actuator, respectively. The length of the link representing the platform of the end-effector is denoted by L_3, (X_1, Y_1) are the coordinates of the base of the RPR kinematic chain, and (X_2, Y_2) are the coordinates of the end-effector for a given posture.

The workspace of kinematic chains of this architecture belongs to one of the same three classes as the RRR kinematic chains. The range of motion of the prismatic joint must be sufficient for the platform to be able to complete

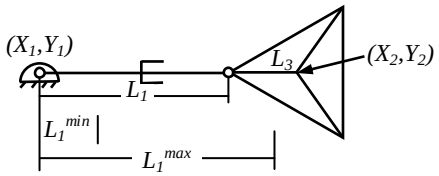

Figure 4: Example RPR kinematic chain

a full rotation for any point inside the workspace. Figures 5 and 6 illustrate the extreme positions and the resulting workspace for kinematic chains of Class 1 and Class 2, respectively. Note that the extreme positions are shown with a reference point on the platform positioned vertically with respect to the fixed revolute joint. Since the relationships that follow are valid for any orientation with respect to the fixed revolute joint, circles are obtained for the workspace limits. In Figures 5 (a) and (b), the reference point on the end effector cannot attain a position if it is outside a circle of radius $L_3 - L_1^{min}$ or $L_1^{max} - L_3$. Thus, the end-effector will only be able to complete a full revolution when the center of the end effector is within a radius defined by the smallest of these two values. In Figures 6 (a) and (b), full revolutions are possible when the end effector is between the two extreme positions shown. From the figures and the above discussion, the radius of each concentric circle that forms the workspace of RPR chains can be determined by the following equation:

$$\begin{aligned} r_1 &= min\{L_3 - L_1^{min}, L_1^{max} - L_3\} \\ r_2 &= L_1^{min} + L_3 \\ r_3 &= L_1^{max} - L_3 \end{aligned} \tag{2}$$

Depending on whether or not the RPR chain respects the following two inequalities, the workspace is defined by different classes.

$$L_1^{min} < L_3 \quad \text{(Inequality A)} \tag{3}$$

$$L_1^{max} - L_1^{min} > 2L_3 \quad \text{(Inequality B)} \tag{4}$$

In Equation (2), when Inequality A is false, radius r_1 becomes negative and there is no workspace of Class 1. For a Class 2 workspace to exist, radius

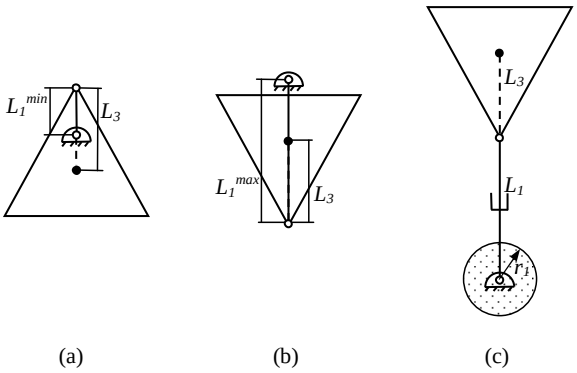

Figure 5: Extreme positions of RPR kinematic chains resulting in a Class 1 workspace

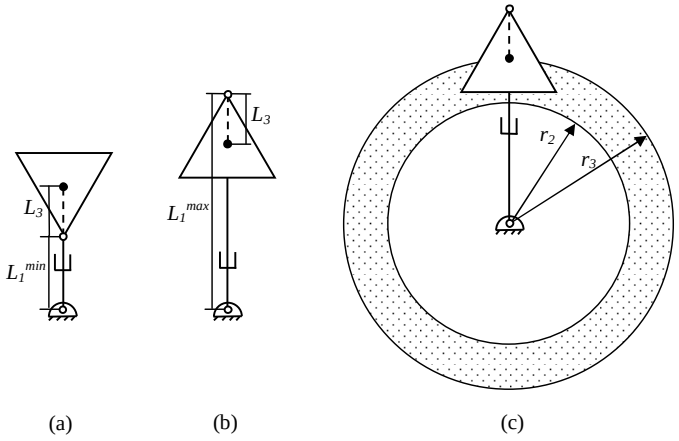

Figure 6: Extreme positions of RPR kinematic chains resulting in a Class 2 workspace

r_3 must be larger than r_2, producing Inequality B. When both inequalities are true, both workspaces exist, producing a Class 3 workspace as shown in Figure 7.

Table 2 summarizes the classes of workspace obtained for every combination of these inequalities.

3.3. Workspaces of Redundant RRRR and RRPR Kinematic Chains

As seen in the two previous sub-sections, the workspaces of the non-redundant portions of RRRR and RRPR kinematic chains are defined by the same three classes. Therefore, the effect of the redundant actuator on the final workspace of these two chain architectures is the same. It follows that the workspaces of manipulators with kinematic chains of either of these

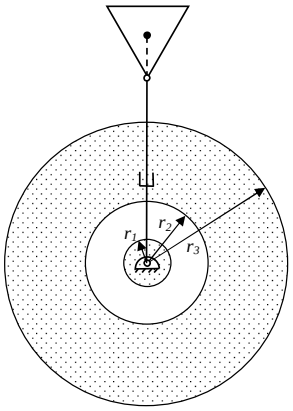

Figure 7: Class 3 workspace

Table 2: Resulting classes in each combination of inequalities A and B

Inequality		**Resulting workspace**
A	**B**	**Class**
True	False	1
False	True	2
True	True	3
False	False	No dexterous workspace

architectures, or even a combination of both, can be determined in the same manner.

The workspaces of redundant RRRR and RRPR kinematic chains are dependent on the class of the non-redundant portion and its associated radii, as well as the length of the redundant link. In Figures 2 and 4, the coordinates (X_1, Y_1) are considered to be fixed. The workspaces of non-redundant RRR and RPR chains are thus centered at this point. However, when the redundant actuator and its link are considered, the center of the workspace is no longer fixed but moves along a circle of radius equal to the length of the redundant link L_4.

Figure 8 shows example RRRR and RRPR kinematic chains. In this figure, the notation for the non-redundant chains is the same as in Figures 2 and 4, while L_4 is the length of the redundant link and (X_3, Y_3) are the coordinates of the base point of the new chain. As stated above, the coordinates (X_1, Y_1) move along a circle of radius L_4 centered at (X_3, Y_3).

For each position of the redundant actuator, the resulting workspace has

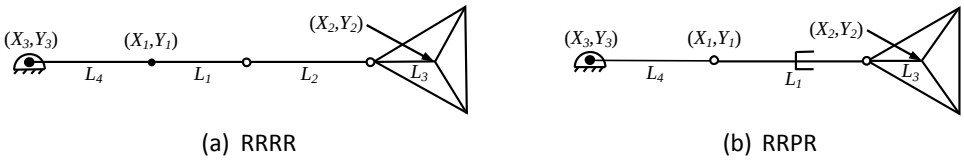

Figure 8: Example RRRR and RRPR kinematic chains

the form of one of the three classes described in the two previous subsections. Therefore, when the coordinates (X_1, Y_1) move, so too does the workspace. Since the redundant actuator can move freely, the workspace of the redundant chain is the union of the workspace of the non-redundant portion at every possible position of the redundant actuator. In other words, the workspaces of the RRRR and RRPR chains are analogous to a marker, the shape of one of the classes discussed above, being dragged along a trajectory defined by a circle of radius L_4 centered at (X_3, Y_3).

3.3.1. Workspace types resulting from Class 1 non-redundant chains

The effect of the redundant actuator is studied considering each of the classes of workspace of the non-redundant portion of the kinematic chain, starting with Class 1. Figure 9 shows the two resulting types of workspace possible with non-redundant chains with a workspace of Class 1. In what follows, workspaces considering the effect of the redundant revolute actuator at the base are defined as Type X, where X indicates the number of circles that define it. In this figure, it can be seen that when L_4 is shorter than the radius r_1, such as in Figure 9(a), only one circle defines the workspace of the redundant chain. However, when L_4 is longer than r_1, a second circle forming an inner boundary is observed. Such is the case of the workspace of Type 2 shown in Figure 9(b). In the figures of this section, the dashed circle shows the trajectory of the center of the non-redundant workspace. Table 3 summarizes the types of workspace, the associated radii and the conditions for workspaces resulting from Class 1 workspaces. In all the results that follow, r_{R0} and r_{R2} indicate inner boundaries while r_{R1} and r_{R3} indicate outer boundaries.

3.3.2. Workspace types resulting from Class 2 non-redundant chains

Figure 10 shows two possible workspaces resulting from Class 2 non-redundant workspaces. It can be seen from this figure that when L_4 is shorter than r_2, the resulting workspace is of Type 2, as can be seen in Figure 10(a).

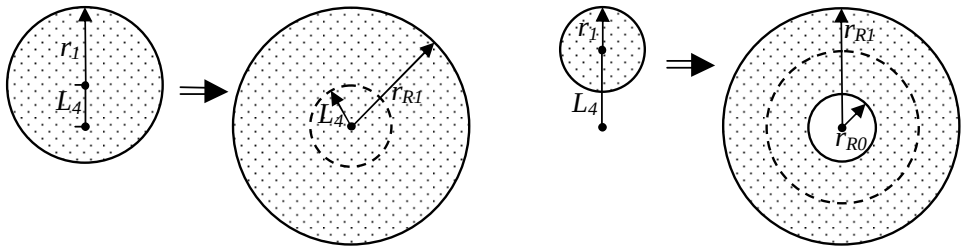

(a) Type 1 (b) Type 2

Figure 9: Workspace types resulting from Class 1 non-redundant workspaces

Table 3: Conditions and radii of the workspace types resulting from Class 1 workspaces

Type	**Condition**	**Radii**	**Figure**
1	$L_4 \leq r_1$	$r_{R1} = L_4 + r_1$	9(a)
		$r_{R0} = L_4 - r_1$	
2	$L_4 > r_1$	$r_{R1} = L_4 + r_1$	9(b)

When L_4 is longer than r_2 but shorter than r_3, the resulting workspace is of Type 1, as seen in Figure 10(b). Finally, when L_4 is longer than r_3, the resulting workspace is of Type 2 again, as seen in Figure 11. Table 4 summarizes the types, the radii and the conditions of workspaces resulting from Class 2 non-redundant workspaces. Note that the definition of r_{R0} in workspaces resulting from Class 1 is slightly different from the one in workspaces resulting from Class 2 (See Tables 3 and 4).

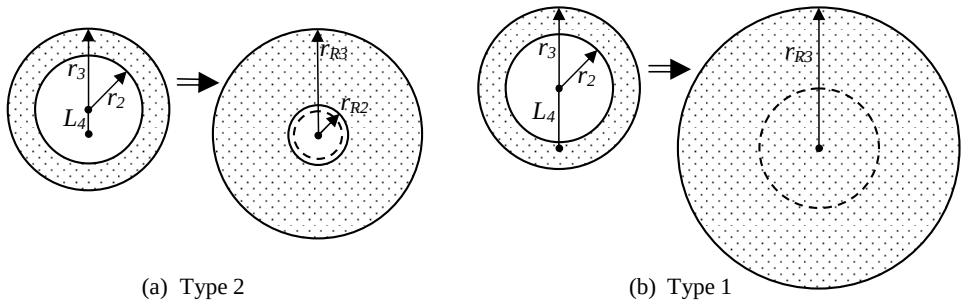

(a) Type 2 (b) Type 1

Figure 10: Workspace types resulting from Class 2 non-redundant workspaces

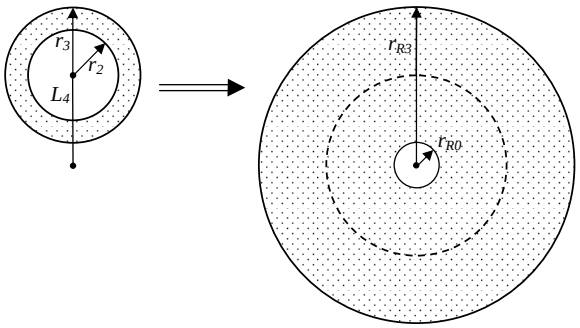

Figure 11: Second Type 2 workspace possible with Class 2 non-redundant workspaces

Table 4: Conditions and radii of the workspace types resulting from Class 2 workspaces

Type	**Condition**	**Radii**	**Figure**
		$r_{R2} = r_2 - L_4$	
2	$L_4 < r_2$	$r_{R3} = L_4 + r_3$	10(a)
1	$r_2 \leq L_4 \leq r_3$	$r_{R3} = L_4 + r_3$	10(b)
		$r_{R0} = L_4 - r_3$	
2	$L_4 > r_3$	$r_{R3} = L_4 + r_3$	11

3.3.3. Workspace types resulting from Class 3 non-redundant chains

The last non-redundant workspace class to be studied is Class 3. Due to the third circle defining this non-redundant workspace, the resulting workspace types can range from a Type 1 to a Type 4, and the conditions that define the types are more complex. In order to gain a better understanding of the relationships that will follow, let us consider the case when L_4 is sufficiently small, and the resulting workspace is a Type 3 as shown in Figure 12.

From the previous discussions, it is readily seen that the radius $r_{R1} = r_1 + L_4$ and that the radius $r_{R2} = r_2 - L_4$. When L_4 increases, so does r_{R1}, while r_{R2} becomes smaller. For the annular non-dexterous workspace to exist, $r_{R1} < r_{R2}$ must be true, or:

$$L_4 < \frac{r_2 - r_1}{2} \tag{5}$$

When L_4 is still inside the region defined by r_1 ($L_4 < r_1$), the annular region can disappear if ($L_4 \geq \frac{r_2 - r_1}{2}$). Combining these two conditions the following is obtained as a necessary condition for no annular region when L_4 is inside the region defined by r_1 :

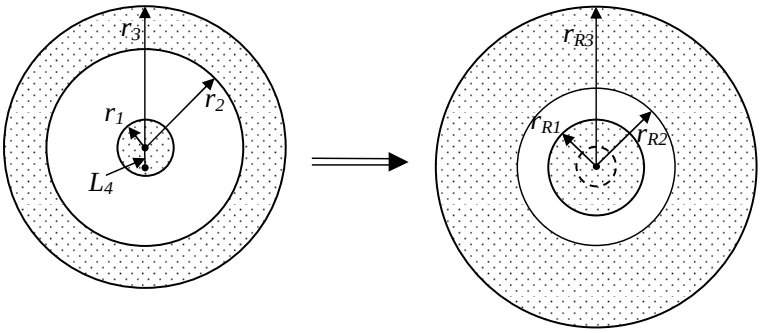

Figure 12: Example workspace of Type 3 resulting from a Class 3 non-redundant workspace

$$r_2 \leq 3r_1 \tag{6}$$

When this condition is true, the workspace will henceforth be considered a Category A while when it is false, the workspace will be considered a Category B. Thus, Category A workspaces will not possess a non-dexterous annular workspace defined by r_{R1} and r_{R2} unless L_4 respects Equation (5). The distinction between the two categories is important since the relationships between L_4 and the radii of the non-redundant workspaces required to define the redundant workspaces are different as will be shown shortly. Figure 13 shows the difference between these two categories of workspace when the redundant actuator is considered.

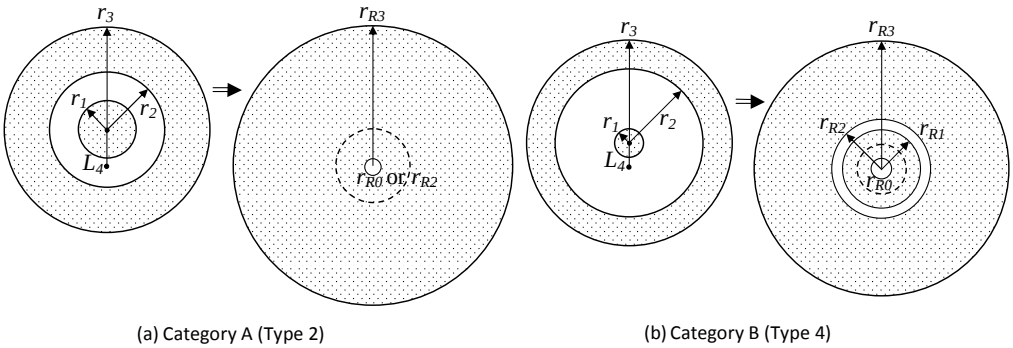

Figure 13: Two categories of Class 3 workspaces

From this figure, the differences between the two categories of Class 3 workspaces can be observed when L_4 is slightly longer than r_1. Recall from previous classes that, in this case, an inner hole can be generated. With

manipulators of Category A, a workspace of Type 4 is not possible because, when L_4 is slightly longer than r_1, the circle of radius r_{R1} has already made contact with the circle of radius r_{R2}, as seen in Figure 13(a). On the other hand, with workspaces of category B the circles of radii r_{R1} and r_{R2} do not make contact even when L_4 is slightly longer than r_1. With workspaces of this category, when L_4 is slightly longer than r_1, the resulting workspace is of Type 4 as seen in Figure 13(b).

Table 5 summarizes the types, the conditions and the radii associated with the workspaces possible from Class 3 non-redundant workspaces of Category A and Table 6 shows the same for Category B workspaces. From these tables, the differences between the two categories of Class 3 workspaces can be readily seen. These tables are ordered in ascending length L_4 to better illustrate the conditions under which each type of workspace is the result of the effect of the redundant actuator. To clarify some of the expressions in the tables, note that when $L_4 > r_1$, the radius of the hole in the inner workspace is the smallest between $L_4 - r_1$ and $r_2 - L_4$ (see Figure 13(a)). They are equal when $L_4 = \frac{r_1+r_2}{2}$.

The transition between each type of workspace in Table 5, from top to bottom of the table, is explained as follows. When Equation (5) is respected, the resulting workspace is a Type 3, as shown in Figure 12. When Equation (5) is no longer respected while L_4 is still inside r_1, the non-dexterous annular workspace disappears, yielding a Type 1 workspace. When L_4 is larger than r_1, an inner hole appears, thus producing a Type 2 workspace. The radius of the inner hole can be either $L_4 - r_1$ or $r_2 - L_4$, depending on whether L_4 has reached $\frac{r_1+r_2}{2}$. When L_4 reaches r_2 and is still less than r_3, the inner hole disappears, yielding again a Type 1 workspace, similar to the one shown in Figure 10(b). Finally, when L_4 is larger than r_3, an inner hole appears, generating a Type 2 workspace similar to Figure 11.

The transition between each type of workspace in Table 6 can be explained similarly. When Equation (6) is not respected, the annular region does not disappear and a Type 3 workspace results when L_4 is less than r_1. When L_4 becomes larger than r_1, an inner hole appears, and as long as L_4 respects Equation (5), the annular region exists, yielding a Type 4 workspace as shown in Figure 13(b). When L_4 no longer respects Equation (5), the annular region disappears, producing a Type 2 workspace with an inner radius that depends on whether L_4 has reached $\frac{r_1+r_2}{2}$ or not. The explanation for the rest of the types is similar to those in Table 5.

Table 5: Conditions and radii of the workspace types resulting from Class 3 workspaces of Category A ($r_2 \leq 3r_1$)

Type	**Condition**	**Radii**	**Figure**
3	$L_4 < \left(\frac{r_2 - r_1}{2}\right)$	$r_{R1} = L_4 + r_1$ $r_{R2} = r_2 - L_4$ $r_{R3} = L_4 + r_3$	12
1	$\left(\frac{r_2 - r_1}{2}\right) \leq L_4 \leq r_1$	$r_{R3} = L_4 + r_3$	
2	$r_1 < L_4 < \left(\frac{r_2 + r_1}{2}\right)$	$r_{R0} = L_4 - r_1$ $r_{R3} = L_4 + r_3$	
2	$\left(\frac{r_2 + r_1}{2}\right) \leq L_4 < r_2$	$r_{R2} = r_2 - L_4$ $r_{R3} = L_4 + r_3$	Similar to 10(a)
1	$r_2 \leq L_4 \leq r_3$	$r_{R3} = L_4 + r_3$	Similar to 10(b)
2	$L_4 > r_3$	$r_{R0} = L_4 - r_3$ $r_{R3} = L_4 + r_3$	Similar to 11

Table 6: Conditions and radii of the workspace types resulting from Class 3 workspaces of Category B ($r_2 > 3r_1$)

Type	**Condition**	**Radii**	**Figure**
3	$L_4 \leq r_1$	$r_{R1} = L_4 + r_1$ $r_{R2} = r_2 - L_4$ $r_{R3} = L_4 + r_3$	12
4	$r_1 < L_4 < \left(\frac{r_2 - r_1}{2}\right)$	$r_{R0} = L_4 - r_1$ $r_{R1} = L_4 + r_1$ $r_{R2} = r_2 - L_4$ $r_{R3} = L_4 + r_3$	13(b)
2	$\left(\frac{r_2 - r_1}{2}\right) \leq L_4 < \left(\frac{r_2 + r_1}{2}\right)$	$r_{R0} = L_4 - r_1$ $r_{R3} = L_4 + r_3$	
2	$\left(\frac{r_2 + r_1}{2}\right) \leq L_4 < r_2$	$r_{R2} = r_2 - L_4$ $r_{R3} = L_4 + r_3$	Similar to 10(a)
1	$r_2 \leq L_4 \leq r_3$	$r_{R3} = L_4 + r_3$	Similar to 10(b)
2	$L_4 > r_3$	$r_{R0} = L_4 - r_3$ $r_{R3} = L_4 + r_3$	Similar to 11

3.4. Workspace of n-RRRR and n-RRPR Manipulator Architectures

Once the workspace geometry of each chain is determined, the next step in the method is to identify all the points where the boundaries of a chain

intersect with the boundaries of the other chains. This is simply done by determining all the points of intersection each circle has with all the circles from the other chains.

Step 3 of the method is then to segment the circles into arcs at each of their points of intersection with the other circles. A circle with n points of intersection is thus divided into n segments. After this step is complete, a list of segments can be drawn for each chain. Each segment is an arc that does not intersect with any other arc of any other chain.

Step 4 of the method is to determine which segments identified in Step 3 are a part of the boundaries of the workspace of the manipulator studied. To determine if a segment is part of the boundaries of the workspace of the manipulator in question, it is verified if the segment is inside the workspace of all the chains from which it does not originate. Since all segments have no intersection with any other segment, if one point of the segment is in the workspace of all other chains, then the entire segment is also in the workspace of all other chains. The mid point on the segment is used for this as it is easy to determine and is farthest to the ends of the segment. This prevents potential errors due to the truncation of computational variables.

The fact that the workspace of each chain is defined by a number of concentric circles simplifies the process of testing whether or not a point is in its workspace. Note that the circles defined by r_{R0} and r_{R2} always define an inner limit to the workspace, i.e., a point in these circles is not in the workspace of the chain. Inversely, circles defined by r_{R1} and r_{R3} define an outer limit to the workspace. It is also important to note that the smaller circles take precedence in this matter. For example, if a point is in both circles defined by r_{R0} and r_{R1}, the circle defined by r_{R0} takes precedence and the point is not in the workspace. Following this logic, one way to determine if a point is in the workspace of a chain is to start with the smallest circle and work outward until the point is in the circle. Then if the first circle to include the point is defined by r_{R0} or r_{R2}, the point is not in the workspace of that chain. If the first circle to include the point is defined by r_{R1} or r_{R3}, the point is in the workspace. If the point is not in any circle, it is not in the workspace.

Once this test is done with all segments with all other chains, a list can be drawn of all the segments forming the boundaries of the workspace of the manipulator in question. At this point in the method, a geometric representation of the workspace of n-RRRR and n-RRPR manipulators is obtained.

Step 5 is used to obtain a scalar value of the area of the manipulator's workspace. The Gauss Divergence Theorem [7] is used to obtain the contribution of each segment that are all added to obtain the area of the workspace [16].

An algorithm was developed in Matlab to implement the proposed method. The inputs required for the algorithm are the coordinates of the fixed revolute joints, the lengths of the links, and the minimum and maximum lengths of the prismatic actuators. The algorithm can handle either n-RRRR manipulators, n-RRPR manipulators, or hybrid n-RRRR-m-RRPR manipulators.

4. Example Workspace

An example of the workspace of a manipulator is presented in this section. The manipulator in question has four chains in total, two of them being of RRRR architecture and the other two of RRPR architecture. Figure 14(a) illustrates this manipulator and Table 7 shows the dimensions of each chain in this manipulator as well as the position of the base of each chain. Figure 14(b) shows the resulting workspace which has an area of 9.0502.

Table 7: Dimensions of the example manipulator

	Kinematic chain			
	1	2	3	4
Type	RRRR	RRRR	RRPR	RRPR
L_1 or L_1^{min}	2.00	1.80	0.20	0.50
L_2 or L_1^{max}	1.20	1.30	2.40	1.60
L_3	0.40	0.40	0.40	0.40
L_4	1.10	0.60	0.90	1.50
(X_3,Y_3)	(0.0 , 1.35)	(2.3 , 2.0)	(2.0 , 0.0)	(0.0 , 0.0)

5. Conclusions

The geometric method presented to determine the geometry of the dexterous workspace for kinematically redundant n-RRRR and n-RRPR planar manipulators is easy to implement. Based on the architectural parameters, the class determining the number of concentric circles of the workspace of the non-redundant chain is identified using Table 1 or Table 2. The associated radii are obtained using Equation (1) or Equation (2). The relationship

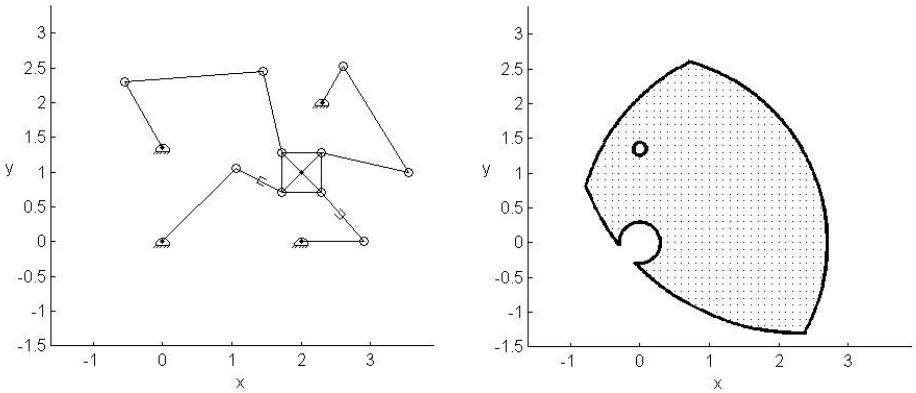

(a) 2-RRRR-2-RRPR (b) Dexterous Workspace

Figure 14: Example workspace of a planar parallel manipulator with a revolute redundant actuator

between the redundant link length L_4 and the radii of the classes dictates the type of workspace as seen in Tables 3-6. The method to determine the boundaries of the intersection of all the kinematic chains is simple since it only involves finding the intersection of circles.

The dexterous workspace of manipulators is an important criterion for their design. With the proposed geometric method, an exact representation of the workspace is obtained. The conditions under which the different types of workspace exist provide useful insight for a designer in the preliminary stages of the design. The implementation of this method is a useful tool in the design of kinematically redundant planar parallel manipulators.

Acknowledgements

The authors would like to thank the Natural Science and Engineering Research Council of Canada (NSERC) for its support in funding this research.

References

[1] V. Kumar, Characterization of workspaces of parallel manipulators, ASME Journal of Mechanical Design 114 (3) (1992) 368–375.

[2] J.-P. Merlet, C. Gosselin, N. Mouly, Workspace of planar parallel manipulators, Mechanism and Machine Theory 33 (1-2) (1998) 7–20.

[3] C. Gosselin, J. Angeles, The optimum kinematic design of a planar three-degree-of-freedom parallel manipulator, ASME Journal of Mechanisms, Transmissions and Automation in Design 110 (1) (1988) 35–41.

[4] R. Williams II, C. Reinholtz, Closed-form workspace determination and optimization for parallel robot mechanisms, in: ASME Design Technology Conferences 20th Biennial Mechanisms Conf., 1988, pp. 341–351.

[5] L. Zhaohui, Y. Zhonghe, Determination of dexterous workspace of planar 3-dof parallel manipulator by auxiliary linkages, Chinese Journal of Mechanical Engineering (English edition) 17 (Suppl.) (2004) 76–78.

[6] C. Gosselin, Determination of the workspace of 6-dof parallel manipulators, ASME Journal of Mechanical Design 112 (3) (1990) 331–336.

[7] R. Buck, Advanced Calculus, International series in pure and applied mathematics, McGraw-Hill Book Company, 1965.

[8] S. Lee, S. Kim, Kinematic analysis of generalized parallel manipulator systems, in: Proceedings of the IEEE Conference on Decision and Control, Vol. 2, 1993, pp. 1097–1102.

[9] K. Zanganeh, J. Angeles, Instantaneous kinematics and design of a novel redundant parallel manipulator, in: Proceedings of IEEE Conference on Robotics and Automation, 1994, pp. 3043–3048.

[10] J.-P. Merlet, Redundant parallel manipulators, Journal of Laboratory Robotic and Automation 8 (1) (1996) 17–24.

[11] J. Wang, C. Gosselin, Kinematic analysis and design of kinematically redundant parallel mechanisms, ASME Journal of Mechanical Design 126 (1) (2004) 109–118.

[12] B. Dasgulta, T. Mruthyunjaya, Force redundancy in parallel manipulators: theoretical and practical issues, Mechanism and Machine Theory 33 (6) (1998) 727–747.

[13] I. Ebrahimi, J. Carretero, R. Boudreau, A family of kinematically redundant planar parallel manipulators, ASME Journal of Mechanical Design 130 (6) (2008) 062306–1– 062306–8.

[14] I. Ebrahimi, J. Carretero, R. Boudreau, Kinematic analysis and path planning of a new kinematically redundant planar parallel manipulator, Robotica 26 (3) (2008) 405–413.

[15] A. Gallant, R. Boudreau, M. Gallant, Dexterous workspace of a 3-PRRR kinematically redundant planar parallel manipulator, Transactions of the Canadian Society for Mechanical Engineering 33 (4) (2009) 645–654.

[16] A. Gallant, R. Boudreau, M. Gallant, Dexterous workspace of a n-PRRR planar parallel manipulators, in: Proceedings of the ASME 2010 IDETC, 2010.